Nonlinear acoustic theoretical model considering acoustic transmissivity in the interior of a real fluid object

Michael Ovando, Jean-Bernard Blaisot, Françoise Baillot

Nonlinear acoustic theoretical model considering acoustic transmissivity in the interior of a real fluid object.

Michael OVANDO, Jean-Bernard BLAISOT*, and Françoise BAILLOT
UMR 6614 - CORIA

Abstract

The present study aims to analyze the response of a fluid system to high-level acoustic pressure fluctuations in Liquid Rocket Engine-like conditions. Propellants are usually in a trans- or super-critical phase during steady-state operative conditions of such engines, which requires special attention to the properties of the fluid. A semi-analitic model is developed to study the interaction between acoustics and an object with properties ranging from sub-critical to supercritical conditions. A particular attention is paid on the acoustic response of the injected fluid that is usually considered as perfectly reflective in sub-critical conditions but where acoustic transmitivity has to be considered in trans- and supercritical conditions. This model consists in the description of both the external velocity potential field (described as the superposition of the incident standing velocity potential field and scattered associated fields) and the velocity potential field inside the object. The first results from this model are presented for a particular condition typical of engine thermodynamic working conditions. The importance of taking into account acoustic transmission in the fluid is shown.

Introduction

The context of this study relies on the thermoacoustic instabilities occuring in Liquid Rocket Engines (LRE). The instabilities results from the coupling between heat release rate fluctuations, $q'(t)$ and pressure fluctuations, $p'(t)$ which usually tune to the chamber's acoustic eigenmodes (Oefelein and Yang, [1]). To understand how these instabilities modify the flow, an approach based on the analysis of the response of a fluid flow to acoustic solicitations is considered. In experiments, this is done by using an acoustic forcing acting on the fluid flow that models injection in engine conditions. In this paper we present an extension of a semi-analytic approach to model the interaction between a liquid or a surpercritical fluid with acoustics.

A theoretical model capable of describing the effects of the acoustic radiation pressure, considering a non-perfectly reflective object (as opposed to how it is seen in the works of Ficuciello [2] and Herrera [3]) is presented. It is based on the approach of Yosioka and Kawasima [4] that expressed the acoustic radiation force on spheres by considering the effects of acoustic transmission inside the object medium.

The next section is devoted to the presentation of the mathematical model. Then follows a presentation of the results when considering a practical injection condition typical of supercritical conditions. A conclusion ends this paper.

Acoustic radiation pressure

A potential acoustic velocity field is considered: $\overrightarrow{u} = -\overrightarrow{\nabla}\Phi_{ext}$. With this convention (Yosioka and Kawasima [4]), the pressure variation in a compressible fluid of density ρ_0 and speed of sound c_0, where acoustic waves are propagated, can be expressed as given by eq. 1 following a development similar to the one of Ficuciello [2].

$$p_{ext} = \rho_0\dot{\Phi}_{ext} - \frac{1}{2}\rho_0(\overrightarrow{\nabla\Phi_{ext}})^2 + \frac{\rho_0}{2c_0^2}\dot{\Phi}_{ext}^2 \qquad (1)$$

The incident field Φ_i is scattered in the presence of an object leading to the scattered field Φ_s. The computation of the resulting field $\Phi_{ext} = \Phi_i + \Phi_s$, is required to estimate the radiation pressure field acting on the surface of the object and the resulting radiation force.

Conventionally, the acoustic radiation pressure is expressed as the time average of equation 1 over a time period of the incident acoustic field.

$$p_{rad} = \frac{1}{T}\int_0^T (\rho_0\dot{\Phi}_{ext} - \frac{1}{2}\rho_0(\overrightarrow{\nabla\Phi_{ext}})^2 + \frac{\rho_0}{2c_0^2}\dot{\Phi}_{ext}^2)dt = p_\zeta + p_\Phi + p_q \qquad (2)$$

where p_ζ is the contribution due to the motion of the object, p_Φ is the time-average volumetric kinetic energy density, p_q is the time-average volumetric potential energy density, and Φ_{ext} is the total velocity potential of the surrounding media

Since we consider the object to be free to move under the influence of the acoustic field, the derivative of the velocity potential referred to the moving origin is given by:

$$\dot{\Phi}_{ext} = \frac{d_U\Phi_{ext}}{dt} - \overrightarrow{U}\cdot\overrightarrow{\nabla}\Phi_{ext} \qquad (3)$$

where $\overrightarrow{U}$ is the barycentric velocity of the object. This velocity can be obtained by applying Newton's second law to the object. The external forces, reduced here to the effect of acoustics, are derived from integration

*Corresponding author: blaisot@coria.fr

over the object boundary, i.e.:

$$m\dot{\vec{U}} = -\iint_S p\,\vec{n}\,dS = \iint_S -\dot{\Phi}_{ext}\rho_0\,\vec{n}\,dS$$

Leading to:

$$\vec{U} = \frac{\rho_0}{m}\iint_S -\Phi_{ext}\,\vec{n}\,dS$$

In the case of a spherical object of radius r_1 and due to the symmetry properties, this results in :

$$\vec{U} = \frac{3\eta}{2r_1}\int_0^{\pi} -\Phi_{ext}\cos(\theta)\sin(\theta)d\theta\vec{e_x} \tag{4}$$

where $\eta = \dfrac{\rho_0}{\rho_1}$ is the ratio between the density of the media and the density of the object. On this study, the index 1 indicates parameters concerning the object, whilst the index 0 indicates the fluid outside of the object.

Doing the time average of equation 3, the term $\dfrac{d_U\Phi_{ext}}{dt}$ reduces to zero and:

$$\langle\dot{\Phi}_{ext}\rangle = -\left\langle\vec{U}\cdot\vec{\nabla}\Phi_{ext}\right\rangle \tag{5}$$

Equation 5 is used in the calculations of p_ζ as:

$$p_\zeta = \langle\rho_0\dot{\Phi}_{ext}\rangle = -\rho_0\left\langle\vec{U}\cdot\vec{\nabla}\ \Phi_{ext}\right\rangle \tag{6}$$

For p_q:

$$p_q = \left\langle\frac{\rho_0}{2c^2}\dot{\Phi}_{ext}^2\right\rangle \tag{7}$$

And finally, the term p_ϕ:

$$p_\phi = \left\langle\frac{1}{2}\rho_0(\vec{\nabla}\Phi_{ext})^2\right\rangle \tag{8}$$

The combination of equations 6, 7 and 8 allows to estimate the acoustic radiation pressure p_{rad} at the surface of the object.

The approach of Yosioka and Kawasima is used here to evaluate the effect of acoustics under trans-critical or supercritical conditions. Indeed, in such conditions, the object interface can no longer be considered as perfectly reflective and the transmission of the acoustical wave inside the object must be taken into account. This is done through the boundary conditions used to compute p_{rad}.

Modelling of velocity potential fields and boundary conditions

We consider a sphere of a given radius r_1 placed at the origin of the coordinate system. The geometry of the problem is reported in figure 1

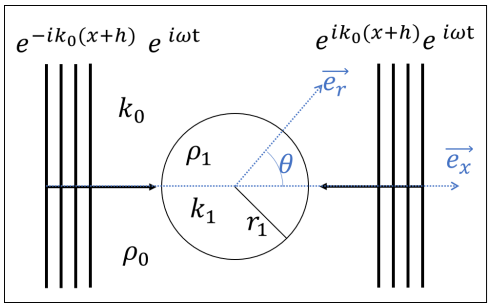

Figure 1: Fluid object (1) with a rigid boundary in a surrounding fluid (0), submitted to an acoustic field. In the case of this study, we consider a standing field

The incident velocity potential Φ_i of the plane standing waves is expressed by:

$$\Phi_i = \frac{\phi_0 e^{i\omega t}}{2}\left[e^{-ik_0(x+h)} + e^{ik_0(x+h)}\right] \tag{9}$$

where $x = r\cos(\theta)$ and $\phi_0 = \dfrac{p_a}{\rho_0\omega}$ is the velocity potential field amplitude, with p_a the amplitude of the associated incident acoustic pressure field, and ω the angular frequency. The velocity potential outside the sphere is written as:

$$\Phi_{ext} = \Phi_i + \Phi_s$$

where Φ_s is the velocity potential of the scattered waves that is expressed as:

$$\Phi_s = \phi_0 e^{i\omega t}\sum_{n=0}^{\infty}(2n+1)(-i)^n A_n\delta_n H_n^{(2)}(k_0 r)P_n(cos\theta) \tag{10}$$

being $H_n^{(2)}$ the spherical Hankel function of the second kind and P_n is the Legendre polynomials. A_n are constants to be determined from the boundary conditions. The term $\delta_n = (-1)^n e^{ikh} + e^{-ikh}$ relates to the position of the object in the acoustic field. Yosioka and Kawasima proposed the following expression for the velocity potential Φ_{int} inside a sphere:

$$\Phi_{int} = \phi_0 e^{i\omega t}\sum_{n=0}^{\infty}(2n+1)(-i)^n B_n\delta_n J_n(k_1 r)P_n(cos\theta) \tag{11}$$

where $k_1 = \omega/c_1$ is the wave number inside the sphere. B_n are other constants determined as A_n from boundary conditions, i.e. by considering the continuity of the radial velocity at the object surface (Eq. 12) as well as the continuity of the pressure (Eq. 13).

$$\frac{\partial\Phi_{ext}}{\partial r} = \frac{\partial\Phi_{int}}{\partial r} \qquad \text{at } r = r_1 \tag{12}$$

$$\rho_0\dot{\Phi}_{ext} = \rho_1\dot{\Phi}_{int} \qquad \text{at } r = r_1 \tag{13}$$

As velocity potential fields are expressed in a base of Legendre polynomials, equations 12 and 13 leads to the following expressions for A_n and B_n:

$$A_n = \frac{\eta k_1 J_n(k_0 r_1) J_n'(k_1 r_1) - k_0 J_n'(k_0 r_1) J_n(k_1 r_1)}{k_0 J_n(k_1 r_1) H_n^{'(2)}(k_0 r_1) - \eta k_1 J_n'(k_1 r_1) H_n^{(2)}(k_0 r_1)} \tag{14}$$

$$B_n = \frac{ik_0/(k_0 r_1)^2}{\left[k_1 J_n'(k_1 r_1) H_n^{(2)}(k_0 r_1) - \lambda k_0 J_n(k_1 r_1) H_n^{(2)'}(k_0 r_1)\right]} \tag{15}$$

Python implementation

All the expressions are implemented in a library *acrad.py*. Since the expressions are given by infinite sums, the convergence is studied to determine the minimum number of terms N_{min} to be considered in the computation. We introduce the reduced acoustic radiation pressure $p^*_{rad}(\theta) = \frac{p_{rad}(\theta)}{\bar{P}}$, where $\bar{P} = \frac{P_{ac}}{\rho_0 c_0^2}$ is the mean acoustic energy per unit volume carried by a standing wave in an environment free from any obstacles. The expression used to calculate the convergence is:

$$error(n) = \max_{0 \le \theta \le 2\pi} \left(|p^*_{n+1}(\theta) - p^*_n(\theta)| \right)$$

The evolution of this error with respect to n is shown in figure 2.

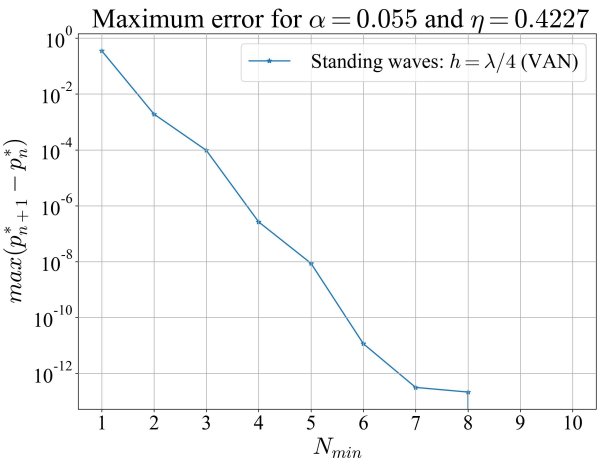

Figure 2: Maximum error on the infinite sums for the calculation of the acoustic radiation pressure evolving in the number N_{min} of terms

The error has been calculated at a velocity antinode (VAN) position in the standing wave acoustic field. We can see a decrease of the error as N_{min} increases. When $N_{min} = 3$, the error is of the order of 10^{-4}. The contribution of the terms over $N_{min} > 8$ is under the floating point precision of the Python code (about 10^{-15}), therefore not contributing to the sum, but just adding computational time to the code. With these results, the truncated number of terms considered for the calculations presented further is $n = 5$, since the error calculated for this value is in the order of 10^{-8}, which is a good compromise between precision and computational cost.

Studying case

The object is placed at a velocity antinode (VAN) where it was previously shown that maximum deformations occurred under the effect of acoustics [2, 3]. The physical parameters used in the calculations are resumed in table 1.

General properties			
T	310 K	P	5 MPa
r_1	0.003 m	f_0	1000 Hz
Acoustic position	VAN ($\lambda/4$)	$\bar{P}$	1000 Pa
Infinite sum terms n	10	Canvas size	250 x 100 pixels
Fluid properties			
Ethane		Nitrogen	
Equation of state	Peng-Robinson	Equation of state	Ideal gas
c_0	358.82 m/s	c_1	108.44 m/s
ρ_0	54.34 kg/m^3	ρ_1	128.53 kg/m^3
k_0	17.51 m^{-1}	k_1	57.94 m^{-1}

Table 1: Physical parameters used in the simulations in this chapter

As indicated in table 1, different equations of state are considered for the calculations of the fluid properties, depending on the fluid considered. For the case of nitrogen, the ideal gas law is used. For the case of ethane, since the studying case is just above its critical point ($P_c = 4.87$ MPa, $T_c = 305.5$ K), the Peng-Robinson equation of state is used:

$$P = \frac{\rho RT}{M - b\rho} - \frac{a\alpha\rho^2}{M^2 + bu\rho M + v\rho^2} \tag{16}$$

with $\alpha = \left(1 + (0.48 + 1.574\Omega - 0.176\Omega^2)\left(\sqrt{\frac{T}{T_c}}\right)\right)^2$, $a = 0.42748\frac{R^2 T_c^2}{P_c}$, $b = 0.08664\frac{RT_c}{P_c}$ $u = 2$, $v = -\rho^2$, and Ω the acentric factor.

The velocity potential fields Φ_{ext} and Φ_{int} are given in figure 3 for the thermodynamic conditions given in table 1 and at a time $t = t_0$ corresponding to the maximum of the instantaneous acoustic velocity at the velocity antinode (VAN). These values represent the amplitude of the velocity potential fields with respect to the maximum amplitude of the incident field when there is no object. On the region of observation, the variation of Φ_{ext} is about 10% of the amplitude of Φ_i. This representation is used to visualize all the involved fields, and following this to calculate each one of the terms of p_{rad}.

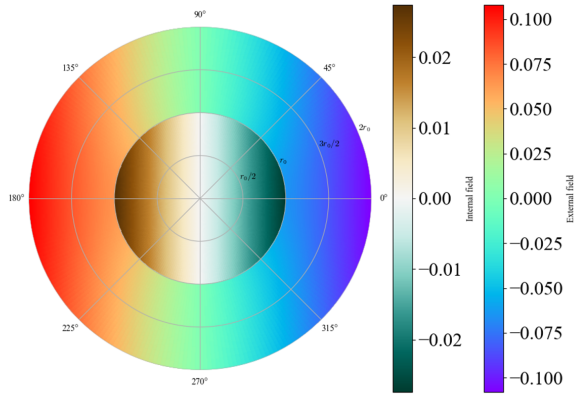

Figure 3: Normalized velocity potential field Φ/ϕ_0 on both the interior (ethane) and exterior (nitrogen) of a sphere at a velocity antinode (VAN), $\eta = 0.4227$, $T = 310$ K and $P = 50$ atm. Time $t = t_0$ corresponds to the maximum instantaneous acoustic velocity at VAN.

On figure 4 we can see the representation of the squared normalized gradient modulus of the external and internal fields at time $t = t_0$. This magnitude is used to represent the volumetric kinetic energy of the system (see equation 8), and since it does not involve the term $\dot{\Phi}_{ext}$, it can be spatially represented. The terms which involve $\dot{\Phi}_{ext}$ (see equations 6 and 7) can only be calculated on the boundary of the object.

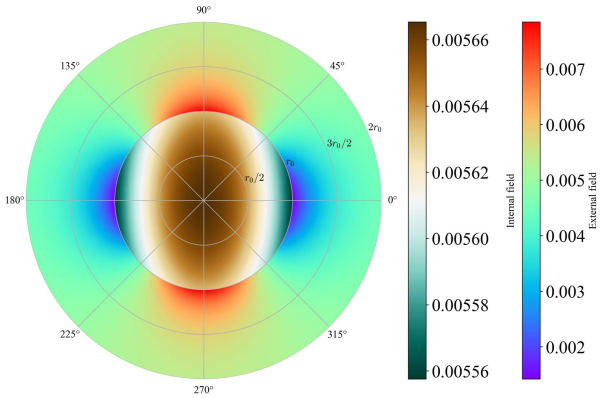

Figure 4: Squared normalized gradient modulus of the external (nitrogen) and internal (ethane) fields $\dfrac{\left|\left|\vec{\nabla}\Phi\right|\right|^2}{\phi_0 k_0}$ at a velocity antinode (VAN), $\eta = 0.4227$, $T = 310$ K and $P = 50$ atm. Radiuses are in meters. Time $t = t_0$ corresponds to the maximum instantaneous acoustic velocity at VAN.

Comparison with prior models

The actual model is compared to the one developed by Ficuciello for perfectly reflective objects. On figure 5, the comparison of p^*_ζ, p^*_Φ, p^*_q and p^*_{rad} as functions of θ is shown for our model (expressed with "trans" for "transmissive") and for Ficuciello's model ("reflect", for "reflective") along the θ axis, for the same physical conditions. For both models, p_q equals zero or about. The other two components p_ϕ and p_ζ, have similar distributions over the object surface but the levels are different between the two models. Globally, the levels are higher for the reflective model with p_ϕ negative and p_ζ positive, resulting in a distribution for p_{rad} varying around zero with positive maximums and negative minimums. In the case of the transmissive model, p_ϕ is also negative and p_ζ positive, but as the levels are lower for both component, it results in negative values for p_{rad} all over the object surface. Also, the amplitude of the variation of p_{rad} over the object surface is larger for the transmissive model. This indicates that the stretching effects that lead the object deformation (not considered here) could be more pronounced with the transmissive model than expected from the reflective model.

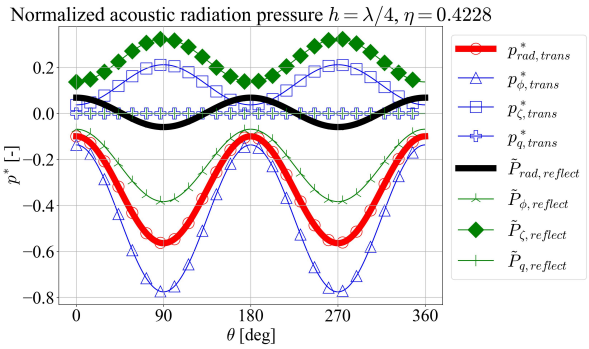

Figure 5: Representation of the normalized acoustic radiation pressure p^*_{rad} and its components p^*_q, p^*_Φ and p^*_ζ for $\eta = 0.4227$ by two models: perfectively acoustically reflective object and acoustically transmissive object. The bold curves indicate the acoustic radiation pressure for the perfectly reflective (in black) and transmissive (in red) object assumption.

Conclusions

The study considered an object at a fixed position in a standing wave acoustic field (velocity antinode, VAN). This position was chosen for its interest relative to potential deformation effects reported in the literature. The implementation of transmission of acoustics in the interior of an object yields a noticeable modification of the prediction of the time-average acoustic radiation pressure distribution over the object surface when compared to reflective models.

A studying case related to engine application was considered, where two fluids: ethane (as the object) and nitrogen (as the surrounding media) are submitted to a standing plane acoustic field at high pressure and temperature conditions. The acoustic radiation pressure was calculated and compared for the case of a perfectly reflective object. Results show a shift of the time-average acoustic radiation pressure with only negative values, and also an increase of the amplitude of the distribution of this acoustic radiation pressure over the object surface. These effects come mainly from the p_ζ term, which is obtained by the barycentric velocity approach we took into consideration. Further studies involving density and speed of sound dependance of the equations, as well as different spatial positioning of the object is

currently being studied.

On the future, deformation of the object is expected to be implemented, by considering different boundary conditions.

Acknowledgements

The authors would like to acknowledge the Centre National des Études Spatiales (CNES) and the Normandy Region for their funding support.

References

[1] J. C. Oefelein and V. Yang, Comprehensive review of liquid propellant combustion instabilities in f-1 engines (1993).

[2] A. Ficuciello, Ph.D. thesis, Université de Rouen Normandie (2017).

[3] R. Herrera, Ph.D. thesis, Université de Rouen Normandie (2022).

[4] K. Yosioka and Y. Kawasima, Acoustic radiation pressure on a compressible sphere, *Acta Acustica united with Acustica* **5**, 167 (1955).